FULL PAPER

Ni_2P Nanoalloy as an Air-Stable and Versatile Hydrogenation Catalyst in Water: P-Alloying Strategy for Designing Smart Catalysts

Shu Fujita, [a] Sho Yamaguchi, [a] Jun Yamasaki, [b] Kiyotaka Nakajima, [c] Seiji Yamazoe, [d] Tomoo Mizugaki,[a] and Takato Mitsudome*[a]

[a] S. Fujita, Dr. S. Yamaguchi, Prof. T. Mizugaki, Dr. T. Mitsudome
Department of Materials Engineering Science, Graduate School of Engineering Science
Osaka University
1-3 Machikaneyama, Toyonaka, Osaka 560-8531 (Japan)
E-mail: mitsudom@chemh.es.osaka-u.ac.jp
[b] Dr. J. Yamasaki
Research Center for Ultra-High Voltage Electron Microscopy
Osaka University
7-1, Mihogaoka, Ibaraki, Osaka 567-0047 (Japan)
[c] Dr. K. Nakajima
Institute for Catalysis
Hokkaido University
Kita 21 Nishi 10, Kita-ku, Sapporo 001-0021 (Japan)
[d] Prof. S. Yamazoe
Department of Chemistry, Graduate School of Science
Tokyo Metropolitan University
1-1 Minami Osawa, Hachioji, Tokyo 192-0397 (Japan)

Supporting information for this article is given via a link at the end of the document.

Abstract: Non-noble metal-based hydrogenation catalysts have limited practical applications because they exhibit low activity, require harsh reaction conditions, and are unstable in air. To overcome these limitations, herein we propose the alloying of non-noble metal nanoparticles with phosphorus as a promising strategy for developing smart catalysts that exhibit both excellent activity and air stability. We synthesized a novel nickel phosphide nanoalloy (nano-Ni_2P) with coordinatively unsaturated Ni active sites. Unlike conventional air-unstable non-noble metal catalysts, nano-Ni_2P retained its metallic nature in air, and exhibited a high activity for the hydrogenation of various substrates with polar functional groups, such as aldehydes, ketones, nitriles, and nitroarenes to the desired products in excellent yields in water. Furthermore, the used nano-Ni_2P catalyst was easy to handle in air and could be reused without pretreatment, providing a simple and clean catalyst system for general hydrogenation reactions.

Introduction

The reduction of polar functional groups, including carbonyl, nitro, and nitrile groups, represents a fundamental and important class of reactions for producing valuable chemicals in niche research and industrial processes.[1,2] In this regard, non-noble metal-based catalysts, such as those based on Ni and Co, play a key role in hydrogenation reactions because of their abundance, low cost compared to platinum group metals (Ru, Rh, Ir, Pd, and Pt), and good activity. Among the non-noble metal catalysts, conventional nickel and/or cobalt sponge catalysts, e.g., Raney catalysts, are often employed for hydrogenation.[3,4] Recently, these catalyst systems have attracted much attention for application in biorefineries and fuel cells.[5,6] However, despite their high efficiency, they also present a critical limitation of pyrophoricity.[7] Hence, they should be prepared under strictly inert conditions with excess NaOH while dissolving Al in the metal alloy, which necessitates a delicate control of conditions; furthermore, their preparation is accompanied by the production of a large quantity of metal wastes. Because of their pyrophoricity, it is difficult to handle activated sponge-metal catalysts during operation, which makes chemical processes complicated; in addition, they are prone to deactivation during long-time storage.[8] Sponge-metal catalysts also suffer from inadequate activity, requiring harsh reaction conditions such as high H_2 pressures for activation.[9] To overcome these drawbacks, supported non-noble metal nanoparticle (NP) systems with good catalytic activity have been proposed.[10,11] However, these catalysts suffer from air-instability and require H_2-pretreatment at high temperatures to generate active metallic states (zero valence) in the NPs. Consequently, from the perspective of practical concerns and green sustainable chemistry, the development of air-stable, highly active, and reusable hydrogenation catalysts that can replace sponge-metal catalysts is highly desirable. In this regard, a successful strategy, "N-doping," was recently reported for the design of air-stable non-noble metal-based NP catalysts by Beller et al.[12–16] The simple pyrolysis of metal complexes with nitrogen-based ligands results

in the production of non-noble metal NPs encapsulated by a nitrogen-enriched graphene layer. The resulting N-ligated metal NPs with a core-shell structure are air-stable and active non-noble metal catalysts that can be used in several hydrogenation reactions. However, the encapsulation of the non-noble NPs shields their active surface sites, and thus, the air stability of the NPs is achieved at the expense of their activity. Therefore, there is considerable interest in eliminating the trade-off between the air stability and activity of non-noble metal NPs.

Combining a metal with another element in NPs is a key strategy for designing novel catalysts. Generally, the second element is also a metal; such metal–metal nanoalloy catalysts have attracted significant attention in a wide range of applications.[17,18] In contrast, the use of metal–non-metal nanoalloys, such as metal phosphide nanoalloy catalysts, has not been studied comprehensively. Few innovative metal phosphide catalysts have been reported in organic synthesis[19–24] despite their high catalytic potential as hydrotreating catalysts, as well as electrocatalysts and photocatalysts for energy conversion.[25–31] In this context, our research group has recently focused on exploring novel catalysis using metal phosphide nanoalloys. We found that non-noble metal phosphide nanoalloys, such as nickel and cobalt phosphides, retain their metal-like states in air and exhibit high catalytic activity for the hydrogenation of biofuranic aldehydes to diketones[32] and of nitriles to amines.[33] On the basis of our studies, we envisaged that alloying non-noble metals with phosphorus (P) would have several merits in organic transformations. The first is the stabilization of the metallic state of the metal species, as an X-ray absorption fine structure (XAFS) study showed that metal phosphide nanoalloys have a metallic state in air (stabilization effect). The second is the modulation of the electronic state of the metal species (ligand effect). Density functional theory calculations revealed that P-alloying can increase the d-electron density of metals near the Fermi level, facilitating hydrogenation.[33] The third is the precise creation of a well-defined catalytic active species in the metal phosphide nanocrystal, which favors selective reactions. In contrast, conventional heterogeneous catalysts have multiple ill-defined active sites, resulting in inferior catalytic performance. These unique properties of metal phosphide nanoalloys strongly motivated us to further investigate their catalytic potential in various organic syntheses.

Herein, we demonstrate that “P-alloying” is a powerful and promising strategy for designing smart catalysts exhibiting high activity and good air stability for efficient and environmentally benign hydrogenation reactions. We synthesized a novel nickel phosphide nanoalloy (nano-Ni_2P) to act as an air-stable and highly active catalyst for the hydrogenation of a variety of carbonyls, nitroarenes, and nitriles using water as the solvent.

Results and Discussion

Preparation and characterization of nano-Ni_2P

nano-Ni_2P was synthesized via a solvothermal reaction between nickel(II) acetylacetonate ($Ni(acac)_2$), hexadecylamine, and triphenylphosphite. The reaction mixture was stirred at 120 °C for 1 h in vacuo before increasing the temperature to 315 °C; while stirring, the system was equilibrated at this temperature in an argon atmosphere for 2 h to produce a black colloidal solution. After cooling to room temperature, the colloidal particles were collected by centrifugation. The obtained solids were washed with a chloroform–acetone solution (1:1, v/v) and dried at room temperature in vacuo to yield black nano-Ni_2P. Using a similar protocol, nano-Ni_5P_4, Co_2P, Cu_3P, and Fe_2P were also synthesized (see Supporting Information (SI) for details). The crystal structure of the nano-Ni_2P was evaluated by X-ray diffraction (XRD) and the corresponding pattern is shown in Figure 1a. The observed diffraction peaks can be indexed to the hexagonal Ni_2P phase.[34] The transmission electron microscopy (TEM) image of the nano-Ni_2P indicates that the nanoalloys had worm-like regular 25 nm-long and 3 nm-wide structures (Figure 1b). Selected area electron diffraction (SAED) patterns (inset in Figure 1b) indicate that the major diffraction rings match well with the hexagonal structure of Ni_2P, further confirming the crystal structure of Ni_2P.[35] Other metal phosphide nanoalloys were also characterized by XRD analysis and TEM observations (Figure S1 and S2, respectively). The elemental distribution of Ni and P in the nano-Ni_2P was determined by high-angle annular dark-field scanning transmission electron microscopy (HAADF-STEM) coupled with energy-dispersive X-ray spectroscopy (EDS) (Figure 1 c–f). Elemental mapping of the nano-Ni_2P confirmed the homogeneous distribution of Ni and P; the molar ratio of Ni and P was calculated to be ~2:1 (Figure S3). These results demonstrate the successful synthesis of uniform worm-like nano-Ni_2P, unlike previously reported sheet-[36] and rod-like[37,38] nano-Ni_2P.

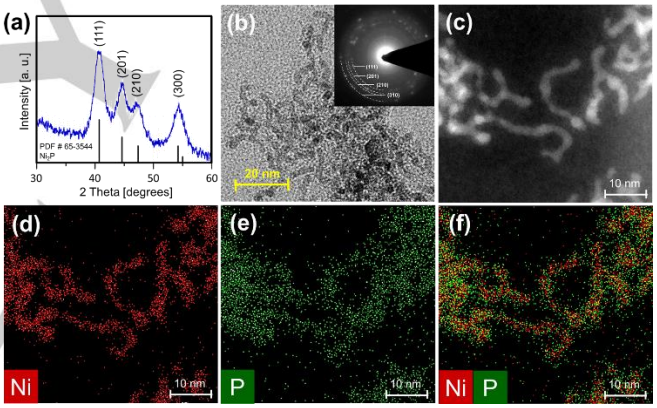

Figure 1. Characterization of nano-Ni_2P with worm-like morphology. (a) XRD pattern of nano-Ni_2P. The reference pattern of Ni_2P (JCPDS card no. 03-0953) is also included in the XRD plot. (b) TEM image of nano-Ni_2P showing a worm-like morphology (the inset shows the corresponding SAED pattern). (c) HAADF-STEM image of nano-Ni_2P. Elemental mapping of (d) Ni and (e) P. (f) Composite overlay image of (d) and (e).

The synthesized nano-Ni_2P was also analyzed using X-ray photoelectron spectroscopy (XPS) to evaluate the electronic state of Ni in the nanoalloy. The obtained Ni 2p spectrum includes peaks at 853.0 and 870.3 eV corresponding to Ni $2p_{3/2}$ and Ni $2p_{1/2}$, respectively, which are close to those of metallic Ni $2p_{3/2}$ (852.8 eV) and Ni $2p_{1/2}$ (870.0 eV) (Figure S4). Subsequently, XAFS analysis was carried out on the nano-Ni_2P in ambient conditions. The X-ray absorption near-edge structure (XANES) spectra of Ni foil, NiO, nano-Ni_2P, and bulk Ni_2P are shown in Figure 2a. The absorption edge energy of the nano-Ni_2P is similar to that of the Ni foil, suggesting that the Ni species in nano-Ni_2P existed in a metal-like state, which is consistent with the XPS results; this unique feature distinguishes the nanoalloy

synthesized in this study from conventional Ni NPs and pyrophoric sponge Ni catalysts. Figure 2b shows the Fourier transform of the extended XAFS (FT-EXAFS) spectra of Ni foil, NiO, nano-Ni_2P, and bulk Ni_2P. The transform function of the nano-Ni_2P exhibits Ni–P and Ni–Ni bonds at 1.7–2.0 and 2.0–2.5 Å, respectively. The absence of peaks corresponding to Ni–O indicates that the nano-Ni_2P do not undergo oxidation in air. The curve-fitting analysis of the FT-EXAFS spectra is shown in Figure S5 and the results are summarized in Table S1. The curve-fitting analysis suggests that the Ni–Ni bond of the nano-Ni_2P is longer than that of the Ni foil (2.58 Å v/s 2.48 Å) because Ni_2P consists of a network of NiP_4 tetrahedra that share vertices. In addition, the $CN_{Ni\text{-}Ni}/CN_{Ni\text{-}P}$ ratio (1.8) of nano-Ni_2P was lower than that of bulk Ni_2P (2.8) (*CN* is the coordination number; the ideal value of $CN_{Ni\text{-}Ni}/CN_{Ni\text{-}P}$ in Ni_2P crystals is 3.0). The low $CN_{Ni\text{-}Ni}/CN_{Ni\text{-}P}$ ratio of nano-Ni_2P can be explained by the exposure of coordinatively unsaturated Ni atoms on the surface. The crystal structure of Ni_2P is shown in Figure 2c; it included crystal planes, such as the (300) plane, in which the Ni(2) content was high. Figure 2d shows the proposed structure of nano-Ni_2P with a (300) plane; the exposure of Ni(2) at the surface is responsible for their low $CN_{Ni\text{-}Ni}$ value. In addition, in these nanoalloys, the Ni–P bonds (Ni(1)–P in Figure 2c) were more rigid than the Ni–Ni bonds (Ni(1)–Ni(2)) because the latter exhibited a large Debye Waller (DW) value (DW > 0.01, Table S1). Therefore, coordinatively unsaturated Ni(2) sites are formed on the Ni_2P nanoalloy surface.

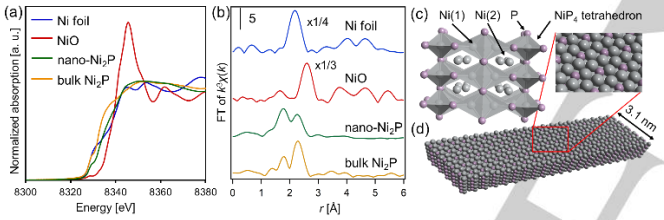

Figure 2. Electronic state and structure of nano-Ni_2P. (a) Ni *K*-edge XANES spectra and (b) Fourier transform k^3-weighted EXAFS of Ni foil, NiO, nano-Ni_2P, and bulk Ni_2P. (c) Crystal structure of Ni_2P. (d) Proposed surface structure of the worm-like nano-Ni_2P with a (300) plane.

Hydrogenation of valuable chemicals using nano-Ni_2P catalysts.

Acetophenone

After studying the morphological, structural, and elemental characteristics of the synthesized metal phosphide nanoalloys, we investigated their catalytic potential for the hydrogenation of acetophenone (**1a**) as a model substrate in water without any additives at 100 °C and 20 bar H_2; the results are shown in Table 1. Among the studied non-noble metal phosphides, nano-Ni_2P showed the highest activity and provided a 16% yield of 1-phenylethanol (**2a**) for 1 h (entry 1). Upon increasing the reaction time to 12 h, **2a** was obtained as the sole product at 97% yield (entry 2). nano-Co_2P also functioned as catalysts for the hydrogenation reaction, but provided a low yield (3%) of **2a** (entry 3), while other metal phosphide nanoalloys (Ni_5P_4, Cu_3P, and Fe_2P) were almost inactive (entries 4–6). Subsequently, we studied the supporting effect of nano-Ni_2P, which exhibited the best catalytic activity among the studied metal phosphides, for the hydrogenation of **1a** in water using different metal oxide supports, which can cooperatively activate reactants with metal nanoalloys.[39] For this purpose, nano-Ni_2P was initially dispersed in hexane and then loaded on different metal oxide supports. The hydrotalcite (HT, $Mg_6Al_2(OH)_{16}CO_3{\cdot}4H_2O$) support was found to significantly enhance the catalytic performance of nano-Ni_2P, resulting in a 93% yield for **2a**, which is a significant improvement compared to that for entry 1 under the same conditions (entry 7). Other oxide supports such as Y_2O_3, ZrO_2, TiO_2, Al_2O_3, and Nb_2O_5 were also effective in producing **2a** at moderate to high yields except for SiO_2 (entries 9–14). It has been reported that carbonyl moieties are activated at the oxygen vacancy sites of HT, which then act as Lewis acid sites.[40] This was confirmed by the Fourier transform infrared (FT-IR) analysis of acetophenone adsorbed on HT; the intense band assigned to C=O stretching vibrations red-shifted from 1708 cm^{-1} to 1691 cm^{-1}, while no such shift was observed after the adsorption of acetophenone on nano-Ni_2P (Figure S6). Thus, the activated C=O moieties in **1a** could then be hydrogenated by the adjacent nano-Ni_2P at the nanoalloy/HT interface.

Table 1. Hydrogenation of acetophenone using metal phosphide catalysts.[a]

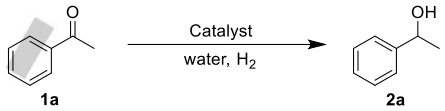

Entry	Catalyst	Yield[b] [%]
1	nano-Ni_2P	16
2[c]	nano-Ni_2P	97
3	nano-Co_2P	3
4	nano-Ni_5P_4	<1
5	nano-Cu_3P	0
6	nano-Fe_2P	0
7	nano-Ni_2P/HT	93
8[d]	nano-Ni_2P/HT	88
9	nano-Ni_2P/Y_2O_3	79
10	nano-Ni_2P/ZrO_2	73
11	nano-Ni_2P/TiO_2	63
12	nano-Ni_2P/Al_2O_3	54
13	nano-Ni_2P/Nb_2O_5	30
14	nano-Ni_2P/SiO_2	7

[a] Reaction conditions: catalyst (5 mol% metal), acetophenone (0.5 mmol), water (3 mL), H_2 (20 bar), 100 °C, and 1 h. [b] Determined by gas chromatography-mass spectrometry (GC-MS) using dimethyl sulfone as an internal standard. [c] 12 h. [d] H_2 (1 bar), 150 °C, 12 h.

Aldehydes and ketones

Non-noble metal catalysts often require harsh reaction conditions to effectively catalyze the hydrogenation of carbonyl compounds (Table S3). In contrast, the nano-Ni_2P/HT was effective even under relatively mild conditions. For example, a high yield of **2a** could be obtained at just 1 bar H_2 (entry 8). Furthermore, the

nano-Ni_2P/HT system could work effectively on a wide range of substrates under 1 bar H_2. Although there are a few reports on the catalytic activity of Ni_2P for the hydrogenation of aldehydes and ketones,[41–45] these compounds require organic solvents and/or suffer from a limited substrate scope (only one or two carbonyls were tested). In sharp contrast, using the nano-Ni_2P/HT system described herein, various aldehydes and ketones, including functionalized aromatic, heteroaromatic, alicyclic, and aliphatic groups, could be efficiently hydrogenated to the corresponding alcohols at excellent yields even at atmospheric H_2 pressure (Figure 3). These facts support our claim that nano-Ni_2P/HT is an air-stable and active catalyst for the hydrogenation of aldehydes and ketones in water.

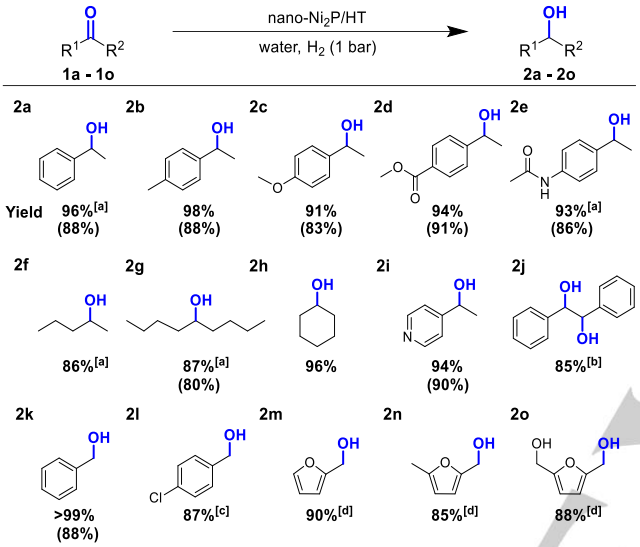

Figure 3. Hydrogenation of aldehydes and ketones catalyzed by nano-Ni_2P/HT. Reaction conditions: nano-Ni_2P/HT (167 mg; 5 mol% Ni), substrate (0.5 mmol), water (3 mL), 150 °C, and 6 h. Yield was determined by GC-MS using dimethyl sulfone as an internal standard. Values in parentheses are isolated yield. [a] Catalyst (333 mg; 10 mol% Ni) and 12 h. [b] Catalyst (333 mg; 10 mol% Ni) and 24 h. [c] 60 °C and 10 h. [d] 100 °C.

Biomass transformation (example: HMF)

We further studied the catalytic activity of nano-Ni_2P/HT in a biorefinery for the transformation of biomass into fuels and valuable chemicals. The hydrogenation of a biomass-derived platform molecule, 5-hydroxymethylfurfural (HMF), to 2,5-bis(hydroxymethyl)furan (BHMF), which is a promising monomer for polyesters and self-healing polymers, is one of the most important biorefinery reactions.[46–48] From a practical standpoint, the transformation of highly concentrated HMF to BHMF in water is challenging because HMF is thermally unstable and is easily oligomerized.[49] It is to be noted that nano-Ni_2P/HT functioned well at an HMF concentration of 20 wt% in water at 60 °C, resulting in a high BHMF yield (Figure 4). Thus, this is the first time that the selective production of BHMF from a concentrated HMF solution could be successfully achieved using a non-noble metal catalyst without base additives or the pre-acetalization of HMF.[50]

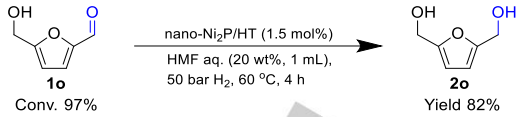

Figure 4. Hydrogenation of aqueous HMF (20 wt%) using nano-Ni_2P/HT as the catalyst.

Recycling experiments (example: acetophenone reaction)

The reusability of heterogeneous catalysts is one of their significant advantages over homogeneous catalysts. In our study, the used nano-Ni_2P/HT could be easily recovered from the reaction mixture by centrifugation and could then be reused without any loss of catalytic activity even after five recycling runs (Figure 5a). We further assessed the reaction rate at 30 min, i.e., before the reaction reached completion, and found that **2a** was obtained in similar yields (♢; Figure 5a) using the used and fresh nano-Ni_2P catalysts. Interestingly, the TEM analysis of nano-Ni_2P/HT after the reaction revealed spherical nano-Ni_2P particles with a mean diameter of 5.9 nm, indicating that the worm-like nano-Ni_2P transformed into spherical nano-Ni_2P during the hydrogenation reaction. This spherical morphology was maintained over five recycling runs (Figure S7). The XRD pattern of nano-Ni_2P and the Ni loading amounts in nano-Ni_2P/HT did not change before and after the reaction (Figure S8 and Table S2). Furthermore, the XAFS results proved that the Ni in nano-Ni_2P/HT retained its metallic nature even after catalysis (Figure S9). To investigate metal leaching, we conducted hot-filtration tests on nano-Ni_2P/HT, as shown in Figure 5b. After filtering out nano-Ni_2P/HT at 50% conversion of **1a**, the filtrate was again treated under similar reaction conditions. However, the new reaction did not yield any products. Inductively coupled plasma-atomic emission spectrometry (ICP-AES) of the filtrate confirmed no leaching of Ni species from the catalyst (the concentration of Ni ions was below the detection limit). These results are highly consistent with the results of recycling experiments and confirm the high durability of nano-Ni_2P/HT catalyst systems.

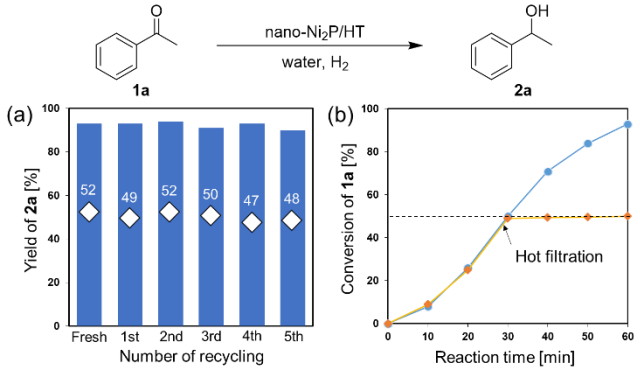

Figure 5. Recycling and hot-filtration experiments. (a) Reuse of nano-Ni_2P/HT for the hydrogenation of acetophenone to 1-phenylethanol. Reaction time: 1 h (blue bars), 30 min (♢). (b) Time course for the hydrogenation of acetophenone using nano-Ni_2P/HT. (●) Without catalyst filtration and (♦) with catalyst removal by hot-filtration after 30 min. Reaction conditions: nano-Ni_2P/HT (167 mg; 5 mol% Ni), acetophenone (0.5 mmol), water (3 mL), H_2 (20 bar), 100 °C.

Nitriles

The high performance of the nano-Ni_2P in water encouraged us to evaluate their catalytic effect for the hydrogenation of nitriles, which is of high significance in the synthesis of primary amines.[51,52] The hydrogenation of valeronitrile was carried out in water in the presence of NH_3 using supported and unsupported nano-Ni_2P at 130 °C and 40 bar H_2, and the observed yields are summarized in Table S4. Unsupported nano-Ni_2P showed the highest activity to afford the corresponding amylamine at a yield of ~89%. Meanwhile, the studied metal oxide supports were ineffective for hydrogenation; instead, they promoted a side-reaction to form alcohols. In addition, the nano-Ni_2P catalysts could work on a broad range of substrates; aromatic, aliphatic, and alicyclic nitriles could be converted to the corresponding primary amines at high yields (Figure 6). To the best of our knowledge, thus far, only sponge Ni[53] and Co(II)/Zn(0)[54] catalysts can function in water for nitrile hydrogenation, but their substrate scope is limited. Hence, nano-Ni_2P represents the first example of non-noble metal catalysts that can work on a broad range of substrates for the hydrogenation of nitriles in water. Notably, nano-Ni_2P efficiently promoted the hydrogenation of benzonitrile (**3a**) to benzylamine (**4a**) under just 1 bar of H_2 (Figure 7), whereas previously reported Ni catalysts inevitably required pressurized H_2.[55–57] This result demonstrates that nano-Ni_2P also functions as a highly active catalyst for the hydrogenation of nitriles under mild conditions.

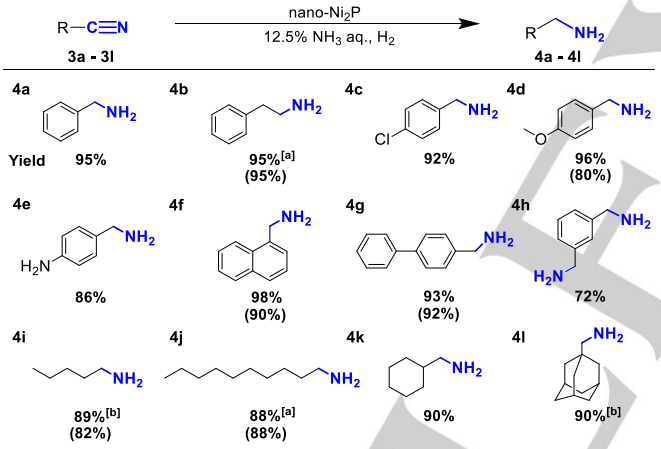

Figure 6. Hydrogenation of nitriles catalyzed by nano-Ni_2P. Reaction conditions: nano-Ni_2P (5 mol% Ni), substrate (0.5 mmol), 12.5% NH_3 aq. (3 mL), H_2 (40 bar), 130 °C, and 3 h. Yield was determined by GC-MS using dimethyl sulfone as an internal standard. Values in parentheses are isolated yield as a hydrochloride salt. [a] 25% NH_3 aq. (3 mL) and 6 h. [b] 6 h.

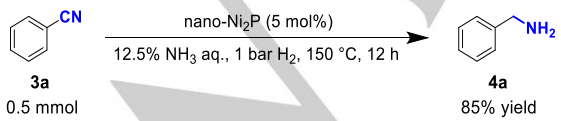

Figure 7. Hydrogenation of benzonitrile using nano-Ni_2P under 1 bar H_2.

Nitroarenes

To demonstrate the generality of the hydrogenation catalysis of nano-Ni_2P in water, they were once again used to catalyze the hydrogenation of nitroarenes. The reduction of aromatic nitro compounds is the most straightforward method for the synthesis of the corresponding aniline derivatives, which are valuable intermediates in the production of agrochemicals, pharmaceuticals, and dyes.[58,59] Although the catalytic activity of nickel phosphide for the hydrogenation of nitroarenes has been reported,[60–62] there is no information available on it in water. The hydrogenation of nitrobenzene in water using supported and unsupported nano-Ni_2P catalysts was studied and the results are shown in Table S5. Interestingly, unsupported nano-Ni_2P showed the highest activity to afford a 94% yield of aniline, whereas nano-Ni_2P immobilized on different supports afforded only low yields. The nano-Ni_2P also exhibited high activity toward various nitroarenes, resulting in anilines at high yields (Figure 8). Notably, a wide range of functional groups, including halogen (**6c** and **6d**), methoxy (**6e**), amino (**6f**), ester (**6g**), amide (**6h**), and hydroxy (**6i**–**6k**) groups, were tolerated under the reaction conditions employed; thus, the highly selective synthesis of functionalized anilines could be achieved. In particular, nano-Ni_2P could catalyze the hydrogenation of methyl 2-nitrobenzoate (**5g**) to methyl 2-aminobenzoate (**6g**), which is used as a bird repellent for food protection and for flavoring medicines, candies, and soft drinks;[63] thus, the green synthesis of **6g** in water could be achieved.

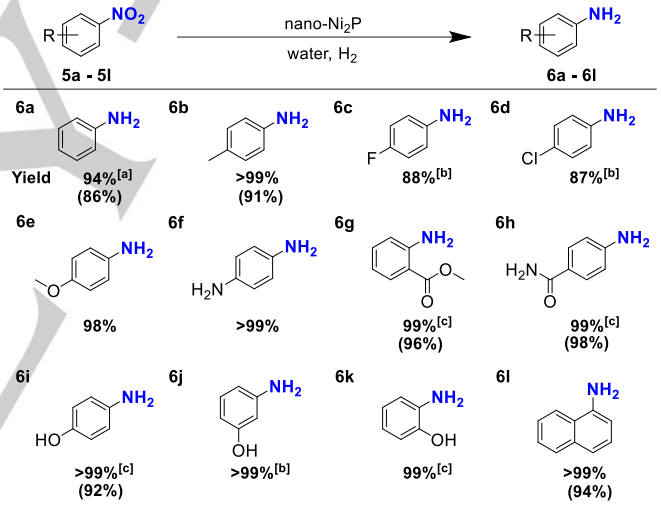

Figure 8. Hydrogenation of nitroarenes catalyzed by nano-Ni_2P. Reaction conditions: nano-Ni_2P (5 mol% Ni), substrate (0.5 mmol), water (3 mL), H_2 (20 bar), 120 °C, and 3 h. Yield was determined by GC-MS using dimethyl sulfone as an internal standard. Values in parentheses are isolated yields. [a] 6 h. [b] H_2 (40 bar), 150 °C, and 6 h. [c] H_2 (40 bar) and 150 °C.

Comparison of catalytic activities of nano-Ni_2P and Raney Ni catalyst for HMF hydrogenation

Finally, to demonstrate the advantages of nano-Ni_2P catalysts over conventional catalysts, we compared the catalytic activities of nano-Ni_2P/HT and sponge Ni for the aqueous-phase hydrogenation of HMF as a model compound. Based on the turnover frequency (TOF), it was observed that nano-Ni_2P/HT exhibited a catalytic activity 22 times higher than that of sponge Ni (Figure 9a). Furthermore, the activation energies required for HMF hydrogenation using nano-Ni_2P/HT and sponge Ni were calculated to 37.9 and 51.4 kJ/mol, respectively, from the slopes of their Arrhenius plots (Figure 9b). These results clearly demonstrate that nano-Ni_2P has a significantly higher catalytic activity and air stability than sponge Ni.

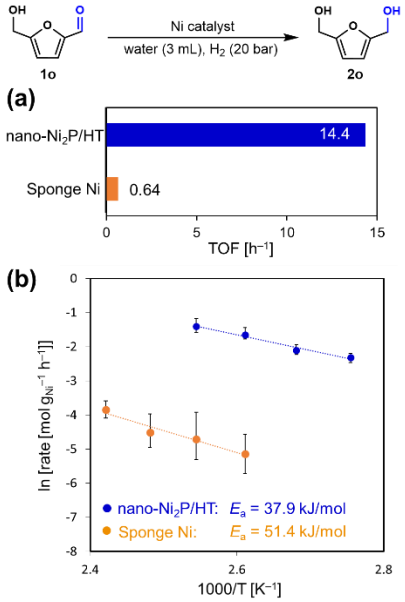

Figure 9. Comparison of catalytic activities of nano-Ni_2P/HT and sponge Ni. (a) TOF of HMF hydrogenation over nano-Ni_2P/HT and sponge Ni catalysts at 120 °C. (b) Arrhenius plot of HMF hydrogenation using nano-Ni_2P/HT and sponge Ni catalysts. TOF was defined as the number of moles of 2,5-bis(hydroxymethyl)furan produced per mole of Ni per hour.

Conclusion

In summary, for the first time, we demonstrated that nano-Ni_2P is an air-stable, highly active, and reusable non-noble metal-based heterogeneous catalyst for the hydrogenation of polar functional groups in water. Aldehyde, ketone, nitrile, and nitroarene groups were efficiently hydrogenated to the corresponding alcohols, amines, and anilines using nano-Ni_2P-based catalysts. XAFS and XPS results revealed that the nano-Ni_2P surface has numerous coordinatively unsaturated Ni active sites and its metallic nature was retained even after reuse in air, demonstrating its high activity and durability. Our results show that "P- alloying" of metal NPs is a powerful strategy to design smart hydrogenation catalysts with good air stability and high activity that can substitute conventional air-unstable non-noble metal catalysts with lower activities. This strategy will be highly useful for developing next-generation green and sustainable chemical processes.

Experimental Section

Synthesis of nano-Ni_2P.

All synthesis reactions were conducted in an argon atmosphere using standard Schlenk line techniques. In a typical reaction, $Ni(acac)_2$ (1.0 mmol) and hexadecylamine (10 mmol) were combined with triphenyl phosphite (10 mmol) in a Schlenk flask. The mixture was stirred at 120 °C for 1 h in vacuo. The reaction temperature was then increased to 315 °C while stirring the mixture and held constant for 2 h to yield a black colloidal solution. The mixture was then cooled to room temperature and the black product was isolated by precipitation in acetone. To remove any organic content, redispersion and precipitation cycles were repeated using a chloroform–acetone (1:1, v/v) mixed solvent. The obtained powder was dried in vacuo overnight.

Preparation of nano-Ni_2P/Support.

Typically, nano-Ni_2P (30 mg) was dispersed in hexane (100 mL) via sonication for 1 h and then stirred with HT (1.0 g) for 6 h at room temperature. The obtained product was dried in vacuo overnight to yield a gray nano-Ni_2P/HT powder. A similar procedure was followed to prepare other nano-Ni_2P/support (Y_2O_3, ZrO_2, TiO_2, Al_2O_3, Nb_2O_5, SiO_2) catalysts. All nano-Ni_2P/support catalysts were characterized by ICP-AES analysis (Table S2) and TEM observations (Figure S10).

Hydrogenation of acetophenone using nano-Ni_2P/HT as the catalyst.

Typically, nano-Ni_2P/HT (0.167 g) was placed in a 50 mL stainless steel autoclave with a Teflon inner cylinder, to which acetophenone (0.5 mmol) and distilled water (3 mL) were subsequently added. The reaction mixture was stirred vigorously at 100 °C at 20 bar H_2 for 1 h. Following the reaction, the autoclave was cooled in an ice-water bath and the hydrogen gas was carefully released. The resulting reaction mixture was diluted with dimethoxyethane and analyzed by GC-MS.

Acknowledgements

This work was supported by JSPS KAKENHI Grant Nos. 26105003, 17H03457, and 18H01790. This study was partially supported by the Cooperative Research Program of Institute for Catalysis, Hokkaido University (19A1002). A part of this work was supported by the "Nanotechnology Platform Program" at Hokkaido University (A-19-HK-0039 and A-20-HK-0011) and Nanotechnology Open Facilities in Osaka University (A-19-OS-0060), Ministry of Education, Culture, Sports, Science and Technology (MEXT), Japan. We thank Dr. Toshiaki Ina (SPring-8) for XAFS measurements (2019A1390, 2019A1649, 2019B1560, and 2019B1858) and Ryo Ota of Hokkaido University for STEM analysis.

Keywords: carbonyl • heterogeneous catalysis • hydrogenation • nickel phosphide • nitrile

[1] S. Nishimura, *Handbook of Heterogeneous Catalytic Hydrogenation for Organic Synthesis*, Wiley, New York, **2001**.
[2] J. D. de Vries, C. J. Elsevier, *The Handbook of Homogeneous Hydrogenation*, Wiley-VCH, Weinheim, **2007**.
[3] M. Raney, US Patent, 1563587, **1925**.
[4] S. H. Tucker, *J. Chem. Educ.* **1950**, *27*, 489–493.
[5] A.-Y. Yin, X.-Y. Guo, W.-L. Dai, K.-N. Fan, *Green Chem.* **2009**, *11*, 1514–1516.
[6] X. Wang, R. Rinaldi, *Energy Environ. Sci.* **2012**, *5*, 8244–8260.
[7] D. Shi, R. Wojcieszak, S. Paul, E. Marceau, *Catalysts* **2019**, *9*, 451.
[8] S. Schouten, D. Pavlović, J. S. Sinninghe Damsté, J. W. de Leeuw, *Org. Geochem.* **1993**, *20*, 901–909.
[9] P. Roose, K. Eller, E. Henkes, R. Rossbacher, H. Höke, *Amines, Aliphatic. Ullmann's Encyclopedia of Industrial Chemistry.* Wiley-VCH, Weinheim, **2015**.
[10] A. Y. Khodakov, W. Chu, P. Fongarland, *Chem. Rev.* **2007**, *107*, 1692–1744.
[11] H. M. T. Galvis, J. H. Bitter, C. B. Khare, M. Ruitenbeek, A. I. Dugulan, K. P. de Jong, *Science* **2012**, *335*, 835–838.
[12] R. V. Jagadeesh, A.-E. Surkus, H. Junge, M.-M. Pohl, J. Radnik, J. Rabeah, H. Huan, V. Schünemann, A. Brückner, M. Beller, *Science* **2013**, *342*, 1073–1076.
[13] L. He, F. Weniger, H. Neumann, M. Beller, *Angew. Chem.* **2016**, *128*, 12770–12783; *Angew. Chem. Int. Ed.* **2016**, *55*, 12582–12594.

[14] D. Banerjee, R. V. Jagadeesh, K. Junge, M.-M. Pohl, J. Radnik, A. Brückner, M. Beller, *Angew. Chem. Int. Ed.* **2014**, *53*, 4359–4363; *Angew. Chem.* **2014**, *126*, 4448–4452.
[15] R. V. Jagadeesh, H. Junge, M. Beller, *Nat. Commun.* **2014**, *5*, 4123.
[16] F. Chen, A.-E. Surkus, L. He, M.-M. Pohl, J. Radnik, C. Topf, K. Junge, M. Beller, *J. Am. Chem. Soc*. **2015**, *137*, 11718–11724.
[17] K. D. Gilroy, A. Ruditskiy, H.-C. Peng, D. Qin, Y. Xia, *Chem. Rev.* **2016**, *116*, 10414–10472.
[18] M. Sankar, N. Dimitratos, P. J. Miedziak, P. P. Wells, C. J. Kiely, G. J. Hutchings, *Chem. Soc. Rev*. **2012**, *41*, 8099–8139.
[19] D. Albani, K. Karajovic, B. Tata, Q. Li, S. Mitchell, N. López, J. Pérez-Ramírez, *ChemCatChem* **2019**, *11*, 457–464.
[20] H. Wang, Y. Shu, M. Zheng, T. Zhang, *Catal. Lett*. **2008**, *124*, 219–225.
[21] Y. Chen, C. Li, J. Zou, S. Zhang, D. Rao, S. He, M. Wei, D. G. Evans, X. Duan, *ACS Catal*. **2015**, *5*, 5756–5765.
[22] S. Carenco, A. Leyva-Pérez, P. Concepción, C. Boissière, N. Mézailles, C. Sanchez, A. Corma, *Nano Today* **2012**, *7*, 21–28.
[23] S. Yang, L. Peng, E. Oveisi, S. Bulut, D. T. Sun, M. Asgari, O. Trukhina. W. L. Queen, *Chem. Eur. J*. **2018**, *24*, 4234–4238.
[24] Y. Zhu, S. Yang, C. Cao, W. Song, L.-J. Wan, *Inorg. Chem. Front*. **2018**, *5*, 1094–1099.
[25] Y. Shi, B. Zhang, *Chem. Soc. Rev*. **2016**, *45*, 1529–1541.
[26] E. J. Popczun, C. G. Read, C. W. Roske, N. S. Lewis, R. E. Schaak, *Angew. Chem.* **2014**, *126*, 5531–5534; *Angew. Chem. Int. Ed*. **2014**, *53*, 5427–5430.
[27] E. J. Popczun, J. R. McKone, C. G. Read, A. J. Biacchi, A. M. Wiltrout, N. S. Lewis, R. E. Schaak, *J. Am. Chem. Soc*. **2013**, *135*, 9267–9270.
[28] M. C. Alvarez-Galvan, J. M. Campos-Martin, J. L. G. Fierro, *Catalysts* **2019**, *9*, 293.
[29] A. Berenguer, T. M. Sankaranarayanan, G. Gómez, I. Moreno, J. M. Coronado, P. Pizarro, D. P. Serrano, *Green Chem*. **2016**, *18*, 1938–1951.
[30] S. T. Oyama, T. Gott, H. Zhao, Y. K. Lee, *Catal. Today* **2009**, *143*, 94–107.
[31] Y. Pei, Y. Cheng, J. Chen, W. Smith, P. Dong, P. M. Ajayan, M. Ye, J. Shen, *J. Mater. Chem. A* **2018**, *6*, 23220–23243.
[32] S. Fujita, K. Nakajima, J. Yamasaki, T. Mizugaki, K. Jitsukawa, T. Mitsudome, *ACS Catal*. **2020**, *10*, 4261–4267.
[33] T. Mitsudome, M. Sheng, A. Nakata, J. Yamasaki, T. Mizugaki, K. Jitsukawa, *Chem. Sci*. **2020**, *11*, 6682–6689.
[34] Y. Pan, Y. Liu, J. Zhao, K. Yang, J. Liang, D. Liu, W. Hu, D. Liu, Y. Liu, C. Liu, *J. Mater. Chem. A* **2015**, *3*, 1656–1665.
[35] Y. Ni, L. Jin, J. Hong, *Nanoscale* **2011**, *3*, 196–200.
[36] Y. Shi, Y. Xu, S. Zhuo, J. Zhang, B. Zhang, *ACS Appl. Mater. Interfaces* **2015**, *7*, 2376–2384.
[37] H. She, Y. Chen, X. Luo, G.-H. Yue, D.-L. Peng, *J. Nanosci. Nanotechnol*. **2010**, *10*, 5175–5182.
[38] B. Seo, D. S. Baek, Y. J. Sa, S. H. Joo, *CrystEngComm*. **2016**, *18*, 6083–6089.
[39] K. Kaneda, T. Mitsudome, *Chem. Rec*. **2017**, *17*, 4–26.
[40] C. Miao, T. Hui, Y. Liu, J. Feng, D. Li, *J. Catal.* **2019**, *270*, 107–117.
[41] R. Gao, L. Pan, H. Wang, Y. Yao, X. Zhang, L. Wang, J.-J. Zou, *Adv. Sci*. **2019**, *6*, 1900054.
[42] J. J. Shi, H. J. Feng, C. L. Qv, D. Zhao, S. G. Hong, N. Zhang, *Appl. Catal. A* **2018**, *561*, 127–136.
[43] D. C. Costa, A. L. Soldati, G. Pecchi, J. F. Bengoa, S. G. Marchetti, V. Vetere, *Nanotechnology* **2018**, *29*, 215702–215709.
[44] P. Yang, H. Kobayashi, K. Hara, A. Fukuoka, *ChemSusChem* **2012**, *5*, 920–926.
[45] P. Liu, Y.-L. Zhu, L. Zhou, W.-H. Zhang, Y.-X. Li, *Catal Lett*. **2020**, 1–8.
[46] M. Kim, Y. Su, A. Fukuoka, E. J. M. Hensen, K. Nakajima, *Angew. Chem.* **2018**, *130*, 8367; *Angew. Chem. Int. Ed*. **2018**, *57*, 8235–8239.
[47] O. Casanova, S. Iborra, A. Corma, *ChemSusChem* **2009**, *2*, 1138–1144.
[48] Z. Zhang, K. Deng, *ACS Catal*. **2015**, *5*, 6529–6544.
[49] X. Tong, Y. Li, *ChemSusChem* **2010**, *3*, 350–355.
[50] J. Wiesfeld, M. Kim, K. Nakajima, E. J. M. Hensen, *Green Chem*. **2020**, *22*, 1229–1238.
[51] J. L. Legras, G. Chuzel, A. Arnaud, P. Galzy, *World J. Microbiol. Biotechnol*. **1990**, *6*, 83–108.
[52] D. Roughley, A. M. Jordan, *J. Med. Chem*. **2011**, *54*, 3451–3479.
[53] J. C. Robinson, H. R. Snyder, *Org. Synth.* **1955**, *3*, 720.
[54] D. Timelthaler, C. Topf, *J. Org. Chem*. **2019**, *84*, 11604–11611.
[55] J. Wang, Q. Tang, S. Jin, Y. Wang, Z. Yuan, Q. Chi, Z. Zhang, *New. J. Chem*. **2020**, *44*, 549–555.
[56] Y. Zhang, H. Yang, Q. Chi, Z. Zhang, *ChemSusChem* **2019**, *12*, 1246–1255.
[57] Y. Cao, L. Niu, X. Wen, W. Feng, L. Huo, G. Bai, *J. Catal*. **2016**, *339*, 9–13.
[58] M. Orlandi, D. Brenna, R. Harms, S. Jost, M. Benaglia, *Org. Process Res. Dev*. **2018**, *22*, 430–445.
[59] J. Song, Z. Huang, L. Pan, K. Li, X. Zhang, L. Wang, J. Zou, *Appl. Catal. B: Environ*. **2018**, *227*, 386–408.
[60] R. J. Gao, L. Pan, H. Wang, X. Zhang, L. Wang, J. Zou, *ACS Catal*. **2018,** *8*, 8420–8429.
[61] P. Liu, Z.-X. Zhang, S. W. Jun, Y.-L. Zhu, Y.-X. Li, *React. Kinet., Mech. Catal*. **2019**, *126*, 456–463.
[62] P. Liu, W.-T. Chang, X.-Y. Liang, J. Wang, Y.-X. Li, *Catal. Commun*. **2016**, *76*, 42–45.
[63] G. Lanzafame, M. Sarakha, D. Fabbri, D. Vione, *Molecules* **2017**, *22*, 619.

Entry for the Table of Contents

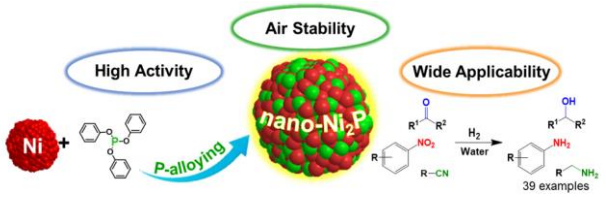

A novel nickel phosphide nanoalloy (nano-Ni_2P) retained its metallic nature in air and exhibited a high activity for the hydrogenation of carbonyls, nitriles, and nitroarenes in water. The used nano-Ni_2P could be easily handled and reused without pretreatment, providing a simple and clean catalyst system for general hydrogenation reactions.